Journal of Materials Chemistry B

Accepted Manuscript

ROYAL SOCIETY OF CHEMISTRY

www.rsc.org/materialsB

Journal Name

ARTICLE

Fluorene–Morpholine-based Organic Nanoparticles: Lysosome-targeted pH-triggered Two-photon Photodynamic Therapy with Fluorescence Switch On-Off

Received 00th January 20xx,
Accepted 00th January 20xx

DOI: 10.1039/x0xx00000x

www.rsc.org/

Moumita Gangopadhyay,[a] Sourav K. Mukhopadhyay,[b] Sree Gayathri,[a] Sandipan Biswas,[a] Shrabani Barman,[a] Satyahari Dey,*[b] N D Pradeep Singh*[a]

Nanocarrier-mediated photodynamic therapy (PDT) is an effective tool for anti-tumour treatment due to targeted and image-guided delivery of photosensitizers (PSs) to diseased tissues. These nanocarriers range from inorganic, ceramic, polymeric to biological nanoparticles (NPs). Such PS-grafted bicomponent nanocarriers have limitations like i) difficulty in surface modification, ii) lower loading percentages of the therapeutic agent, iii) unstable physical encapsulation etc. By any means, if we can prepare PSs directly as NPs then we can surpass the above drawbacks. Hence, we synthesised new two-photon fluorene-functionalised morpholine (Fluo-Mor)-based organic NPs that showed strong fluorescence and profound photodynamic therapy (PDT) activity only in acidic medium. Such pH-responsive appearance of fluorescence enables Fluo-Mor NPs for real time monitoring of photodynamic therapeutic activity selectively in low-pH organelles viz. lysosome. Cytotoxicity of Fluo-Mor NPs was monitored using time-dependent and dose-dependent cancer cell viability assay and confocal imaging.

Introduction

Photodynamic therapy (PDT), a non-invasive therapeutic modality, is an effective modern technique for anticancer treatment.[1] PDT involves irradiation of a photosensitizer (PS), mostly in the region of visible or near-IR (NIR), in presence of molecular oxygen. Hence, it has minimum side effects on normal tissues. Despite these advantages, clinical PDT agents are few due to their lack of specificity, which leads to undesired toxicity and prolonged skin photosensitization.[2] Moreover, most PS molecules give decreased quantum yield due to their hydrophobic nature leading to self-aggregation.[3] Therefore, to increase the solubility and to avoid off-target exposure of PSs in physiological system, nanoparticle (NP)-mediated PS delivery has gained much attention.

NPs have special features like significant hydrophilicity, enormous surface areas that can be appropriately functionalized leading to various chemical or biochemical properties, and efficient tissue penetration ability through fine capillaries and epithelial lining because of their sub-micron and sub-cellular size.[4] Of late, there has been remarkable development in PS-loaded NPs viz. surface-functionalized ceramic NPs, metallic NPs, physical encapsulation within polymeric NPs and micelles, etc.[5-8] Although such nanocarriers render immense advantages in delivering PSs for targeted cancer treatment, some of these suffer from some crucial shortcomings e.g. lower loading capacity, undesired toxicity, unstable physical encapsulation etc.[9-14] Though recent reports on formulation of Au25(SR)−18 clusters in conjugation with upconversion nanoparticles[15] or Fe3O4/ZIF-8-Au25[16] based MOF render immense advantages in the field of anticancer treatment in terms of multimodal therapeutic activity, photoacoustic and MRI imaging, these nanocarriers include crucial synthetic procedures. Thus, formulating organic photosensitizers (PSs) directly as NPs by simple reprecipitation technique can possibly overcome such limitations.

In 2005, Barbara et al reported synthesis of perylenedicarboximide organic NP leading to a multichromophoric system with dual emission property.[17] Further, Rahimi et al prepared porphyrin NPs by ultrasonic method and studied their optical properties.[18] However, such porphyrin NPs were found to display effective catalytic property only in presence of metal ions. Recently, our group reported perylene organic NPs for light-triggered anticancer drug release.[19] Prerequisites of formation of organic NPs with desired size and shape are extended π-conjugation, optimum hydrophobicity etc.[20]

Although, few reports exist on synthesizing PS nanocrystals for PDT,[21-23] there is scope for exploring new PS NPs for targeted and image guided cancer treatment. This encouraged us to directly fabricate organic NPs of a well-known PS. For the

[a] Department of Chemistry, Indian Institute of Technology Kharagpur 721302, West Bengal, India, E-mail: ndpradeep@chem.iitkgp.ernet.in
[b] Department of Biotechnology, Indian Institute of Technology Kharagpur 721302, West Bengal, India, E-mail: sdey@hijli.iitkgp.ernet.in

Electronic Supplementary Information (ESI) available: Synthesis and characterization of Fluo-Mor, quantum yield calculations, ^{1}HNMR, ^{13}CNMR, UV, fluorescence spectra of Fluo-Mor are discussed in supplementary material of this paper. See DOI: 10.1039/x0xx00000x

current study, we selected fluorene derivative because of their unique features like (i) strong 2PE-induced PDT utilizing the NIR spectral region, (ii) extended π-conjugation, and (iii) moderate hydrophobicity.[24] Further, we also functionalized the fluorene derivative with a morpholine unit which served the following purposes; (i) pH-triggered PDT, as morpholines could behave as a donor moiety indulging in effective photoinduced electron transfer (PET) to the acceptor fluorene derivative at neutral pH, (ii) morpholines are known to be specific to the acidic organelles e.g. lysosomes (pH 4.0–6.0) of the cells,[25] (iii) pH-regulated fluorescence emission for real time monitoring of the PDT action by the state of the art NPs. Thus, we can observe a synergic effect of real-time monitoring and on-demand pH-triggered PDT by Fluo-Mor organic NPs minimizing undesirable toxicities as presented in **figure 1**.

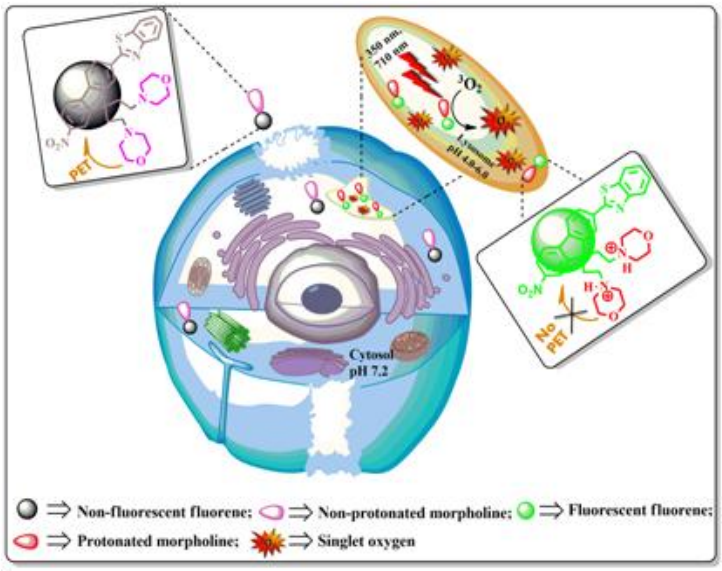

Figure 1 Schematic representation of pH-triggered lysosome targeted Photodynamic therapy (PDT) by Fluo-Mor organic nanoparticles

Experimental Section

Synthesis of Fluo-Mor (7)[26]

A mixture of compound **6** (0.050 g, 0.145 mmol) (**scheme 1**), 4-(2-bromoethyl)morpholine (0.028 g, 0.145 mmol), KI (0.003 g, 0.015 mmol), and DMSO (5 mL) was stirred at room temperature, to which powdered KOH (0.034 g, 0.61 mmol) was slowly added under N_2. The colour of the reaction mixture changed from bright yellow to dark green immediately after KOH addition, and, after 1h, the reaction mixture was poured into water and extracted with hexanes. The organic extract was washed with water, dried over Na_2SO_4, and concentrated, affording 0.040 g dark brown crude. Purification was accomplished using flash column chromatography (230-400 silica gel) with 30 % EtOAc/hexanes, providing 0.030 g of dark yellow solid (70 % yield). FTIR (KBr, cm^{-1}): 1190, 1438, 1720, 2925. UV-vis (citrate buffer): λmax (log ε): 350 (0.55). ^{1}H NMR (200 MHz, $CDCl_3$): 8.43 (s, 1H), 8.36-8.32 (d, 1H, J = 8.4 Hz), 8.31-8.27 (d, 1H, J = 8 Hz), 8.023 (s, 1H), 8.00-7.85 (m, 3H), 7.66-7.62 (d, 1H, J = 8 Hz), 7.42-7030 (m, 2H), 4.05-4.00 (t, 8H, J = 5 Hz), 2.51-2.49 (t, 4H, J = 1.2 Hz), 2.21-2.18 (t, 8H, J = 2.2 Hz), 1.65-1.64 (t, 4H, J = 1.8 Hz). ^{13}C NMR (50 MHz, $CDCl_3$): 166.5, 152.21, 147.93, 147.20, 142.3, 139.40, 136.08, 134.69, 131.61, 129.69, 129.05, 124.93, 123.45, 115.98, 114.20, 111.94, 109.3, 67.61, 63.11, 51.31, 43.37, 40.07, 14.25. For $C_{32}H_{34}N_4O_4S$ [MH+] = 571.2301, found 571.2303.

Synthesis of Fluo-Mor NPs

Reprecipitation technique was followed to synthesize Fluo-Mor NPs.[18] To a vial containing 20 mL millipore water, 10 µL of 3 mM solution of Fluo-Mor conjugate in acetone was slowly added at room temperature under controlled stirring. The size and shape of the Fluo-Mor NPs was verified by UV/vis, fluorescence, TEM, DLS and zeta potential measurements.

Photophysical properties of Fluo-Mor NPs

Measurement of pH dependent fluorescence quantum yield

The fluorescence quantum yield of the Fluo-Mor NPs in different pH solutions was determined by reference point method taking Quinine sulfate in 0.1 M H_2SO_4 (literature quantum yield: 54%) as a standard sample. The detailed experimental procedure has been discussed in supporting information (**section 4.1**).

Photochemical properties: pH-dependent singlet oxygen generation[2,27]

In order to confirm pH dependence of the generation of singlet oxygen by Fluo-Mor NPs, we recorded the photodegradation rate of 1,3-diphenylisobenzofuran (DPBF, Aldrich) in presence of the NPs in varied pH solutions. The singlet oxygen quantum yield (Φ_Δ) was determined in citrate buffer solutions of different pH values containing 0.5 % DMSO and taking Rose Bengal as the reference having a singlet oxygen quantum yield of 0.74 in water.

Lysosome specific cellular internalization studies of Fluo-Mor NPs in human Colon cancer cell HT-29[28]

To study the lysosome targeting of Fluo-Mor NPs, Human Colon cancer HT-29 cells (10^5cells/well) were incubated with Fluo-Mor NPs with different concentrations (75, 100 300 µg/mL) for 4 h in a humidified 5% CO_2 atmosphere at 37 °C cell culture medium. Following 4 % paraformaldehyde treatment and washing several times with PBS buffer (1X, pH 7.4), the colon cancer cells were stained with LysoTracker Red DND-99 (100 nM) and further incubated for 1 h at 37 ºC. After washing the cells with PBS buffer, imaging was done using an Olympus FV1000 confocal microscope with the appropriate filter. Experimental details have been discussed in supporting information (**Section 5.1**).

Photoinduced cytotoxicity of Fluo-Mor NPs by MTT assay[29]

Cytotoxicity of Fluo-Mor NPs with and without irradiation on human colon cancer HT29 cells was determined by conventional MTT assay (**supporting information section 5.2**). Fluo-Mor NPs treated cells were incubated for 4 h. Afterwards, the cells were irradiated with UV/vis light of wavelength ≥365 nm (0-5 min) and further incubated for about 16 hours at 37 °C. Following treatment for 16 hrs at 37 °C, MTT solution (5mg/ml in PBS) was added and incubation was prolonged for

5 h at 37 °C. Inhibition of cell proliferation was monitored by MTT (Himedia) assay. Further the cell death pathway was monitored by Live/dead assay[30] with Calcein AM, Ethidium Homodimer 1 and nuclear morphological studies with DAPI[31] as has been discussed in **supporting information section 5.3 and 5.4** respectively.

Intracellular singlet oxygen generation by Fluo-Mor NPs[32]

HT-29 cells treated with Fluo-Mor NPs were washed with PBS and then incubated with 4 µL of 10 mM DCFH-DA stock solution in PBS solution for 30 min. After washing cells were irradiated with a medium pressure mercury lamp with suitable 0.1 M $CuSO_4$ solution as filter (≥365 nm) (16 mW cm^{-2}) for 5 min and further incubated for 16 h. After washing with Dulbecco's modified eagle medium (DMEM), the fluorescence signal was determined by a Olympus FV1000 confocal microscope with excitation at 488 nm and emission at 530 nm (**supporting information section 5.4**).

Results and Discussions

Synthesis of Fluo-Mor (7)

Synthesis of Fluo-Mor i.e. fluorene derivative attached to morpholine moiety was carried out following a slightly modified version of a reported procedure[26] (**scheme 1**). Commercially available fluorene (**1**) was first nitrated in presence of AcOH and conc. HNO_3, followed by iodination with KI and I_2 leading to 2-iodo-7-nitro fluorene (**3**). Refluxing compound **3** for 1.5 h in presence of CuCN and $FeCl_3$ yielded compound 4, which in turn was hydrolysed to 7-nitro-9H-fluorene-2-carboxylic acid (**5**). Further reaction between the acid chloride of **5** and 2-aminothiophenol in presence of NMP at 100–110 °C led us to 2-(7-nitro-9H-fluoren-2-yl)benzo[d]thiazole (**6**). Finally, compound 6 was stirred with 4-(2-bromoethyl)morpholine in presence of KOH and KI at room temperature for 1 h to afford the desired Fluo-Mor (**7**). The UV-Vis, FT-IR, ^{1}H NMR, ^{13}C NMR spectra of the synthesized compounds are provided in supporting information (**supplementary fig. S1–S2**).

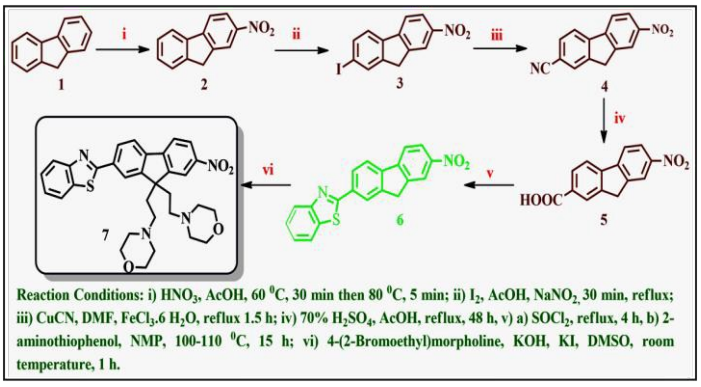

Scheme 1 Synthesis of desired compound Fluo-Mor (**7**)

Synthesis and Characterization of Fluo-Mor organic NPs

Next, uniform, globular and non-aggregated NPs of Fluo-Mor were prepared by reprecipitation technique.[18] Solution of Fluo-Mor in acetone was added slowly into deionized water under constant ultra sonication at room temperature. Ultra sonication was maintained throughout the addition procedure to allow proper mixing of the two solvents. The nanoparticles were generated by diffusion of acetone in deionized water. This resulted in a drop of the interfacial tension between the two phases causing an increase of the surface area and the instantaneous precipitation of nanoparticles. TEM, DLS studies (**figure 2a-c**) of the as-synthesized Fluo-Mor NPs suggested that the size of the NPs was ~ 43 nm, thus can be well internalized into tumour cells for *in vitro* and *in vivo* diagnosis and treatments. The polydispersity index of thus-prepared Fluo-Mor NPs was 0.002 at 43.82 nm, implying uniformity of the nanoparticles. Variations in average size of the Fluo-Mor NPs with change in solution pH were also monitored (**supplementary fig. S4**). The average diameter of Fluo-Mor NPs gradually increased upon decreasing the pH, which is in accordance with literature reports.[33,34] Zeta potential values for the as-synthesized NPs were found to become largely positive upon lowering of the pH (**figure 2d**),[35] due to protonation of the morpholine nitrogen atom at lower pH. Such selective switching of charge from negative to positive under acidic environment enhances the therapeutic effects of Fluo-Mor NPs specifically in tumour cells.[36-38] Of late, researchers have utilized drug delivery vehicles that are negatively charged at neutral pH but acquire positive charge at lower pH. Positively charged carriers interact strongly with serum components leading to fast clearance; however, negatively charged species showed prolonged circulation time due to lack of interaction with blood components. Such carriers that are inert throughout blood circulation can deliver the drug to the endosomal/lysosomal compartments of cancer cells. Ghinea et al proved that presence of some positively charged part on the cell surface favoured internalization of negative species over neutral species.[39] Thus, the charge reversal attribute of Fluo-Mor NPs enables them to act as endosomolytic and lysosomolytic pH-responsive PDT agent. Further, the Fluo-Mor NPs were stable under physiological condition even after 7 days (**supplementary Table S1**).

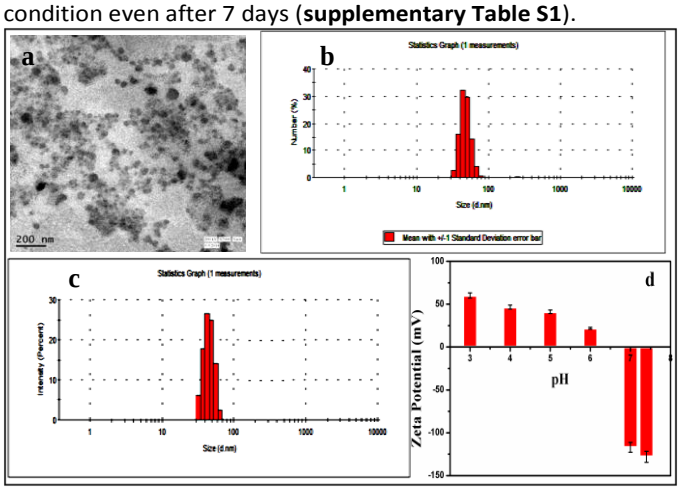

Figure 2 (a) TEM, **(b)** DLS presented in terms of number percentage, **(c)** DLS presented in terms of intensity percentage and **(d)** pH-dependent Zeta Potential study of Fluo-Mor organic NPs

pH-dependent photophysical studies of Fluo-Mor organic NPs

The pH-dependent UV and fluorescence studies also indicated the protonation of the morpholine unit at acidic pH **(figure 3a-b)**. As shown in **figure 3b**, fluorescence intensity decreased on increasing the pH from 3 to 7.4 due to the ongoing PET process in Fluo-Mor at neutral or alkaline pH. At higher pH, morpholine behaves as a donor moiety to the acceptor fluorene due to the presence of a lone pair of electrons on nitrogen. Hence, the intrinsic fluorescence of fluorene moiety is quenched. However, at lower pH, the morpholine nitrogen unit is protonated such that PET is stopped and fluorescence is enhanced. In addition, the appearance of strong fluorescence at lower pH can also be due to the aggregation of Fluo-Mor NPs, as pH-dependent DLS studies of Fluo-Mor NPs showed increased hydrodynamic size at lower pH values (**supplementary fig. S4**). According to previous reports, various other fluorene derivatives also showed such aggregation due to the presence of conjugated donor-π bridge-acceptor moieties as present in Fluo-Mor NPs.[40-42] **Figure 3c** shows the gradual pH-dependent change in fluorescence intensity under fluorescence lamp. **Figure 3d** represents the reversible switching on and off process of fluorescence. Further, fluorescence quantum yield values for Fluo-Mor at different pH values were also calculated and the quantum yield values were found to decrease with increasing pH (from pH 3 to pH 7.4) (**supplementary Table S2**). We also compared the effect of other inorganic metal ions and hydrophobic serum protein on the fluorescence properties of Fluo-Mor NPs. No significant variation in fluorescence intensity of Fluo-Mor NPs was observed in absence and presence of excess of those elements (**supplementary fig. S5**), which implied high selectivity of Fluo-Mor NPs towards acidic environment.

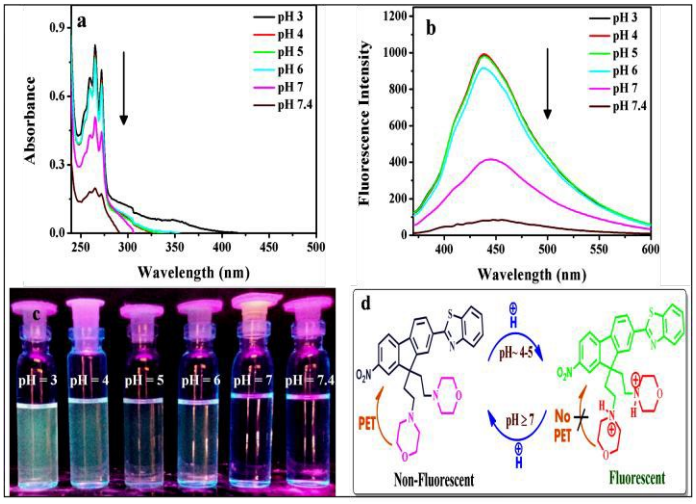

Figure 3 (a) UV, **(b)** Fluorescence spectra of Fluo-Mor (70 μM) in citrate buffer solutions with different pH, **(c)** Fluorescent images of Fluo-Mor at different pH values under fluorescence lamp and **(d)** Mechanism of fluorescence quenching

pH-dependent singlet oxygen generation ability of Fluo-Mor organic NPs

The photosensitizing property i.e. singlet oxygen generation ability of Fluo-Mor NPs was also found to be dependent on the pH of the environment. The singlet oxygen generation property was monitored following the well-known 1,3-diphenylisobenzofuran (DPBF) degradation study at varying pH (**figure 4**).[2,27] Equimolar mixtures of DPBF (34 μM) and Fluo-Mor NPs (35 μM) in citrate buffer solutions containing 0.5 % DMSO were irradiated under both 1PE (≥365 nm) and 2PE (740 nm) for 5 min and 15 min respectively. The $^1O_2$ quantum yields (**Table 1**) decreased with increasing pH of the solution. Maximum quantum yield was found in the region pH 3.0–4.0 (Φ_Δ = 0.65 and 0.58, respectively), whereas the value decreased to 0.09 at pH 7.4. Hence, the generation of $^1O_2$ by the Fluo-Mor NPs was almost negligible at physiological pH of non-cancerous cells. The values of singlet oxygen quantum yields of some standard photosensitizers in a similar pH-controlled process reported in recent times range from 0.37 for a tetraamino silicon(IV) phthalocyanine moiety[43] to 0.53 for a porphyrin derivative[44] and 0.56 for zinc phthalocyanine[45]. Thus, Fluo-Mor NPs in the present work showed comparable Φ_Δ with respect to all these conventional photosensitizers. Photoinduced singlet oxygen generation from Fluo-Mor NPs were also calculated using 740-nm diode laser for 2 PE and similar trend for singlet oxygen quantum yield was found (**supplementary fig. S6, Table S3**).

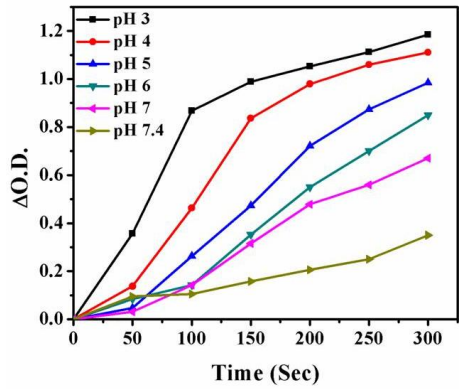

Figure 4 Photodegradation study of DPBF (418 nm) in presence of Fluo-Mor NPs at different pH

Table 1 Singlet oxygen quantum yield of Fluo-Mor NPs at different pH values

pH (in Citrate Buffer solution containing 0.5 % DMSO)	Φ_Δ[a]
3	0.65
4	0.58
5	0.35
6	0.32
7	0.25
7.4	0.09

[a]Rose Bengal as reference with known Φ_Δ = 0.74 in water

Lysosome specific cellular internalization studies of Fluo-Mor NPs in human colon cancer cell HT-29

To establish the in vitro application of the PDT efficacy of Fluo-Mor NPs, initial cellular internalization studies were carried out in human colon cancer cell line, HT-29 through confocal microscopy. To prove lysosomal targeting ability, the human colon cancer cell line was incubated with Fluo-Mor NPs in presence of the lysosome-staining dye LysoTracker Red® DND 99.[28] The confocal images showed efficient co-localisation of the Fluo-Mor NPs and the lysotracker dye, which was indicated by the overlap between the green fluorescence of Fluo-Mor NPs and the red fluorescence of the lysotracker dye (**figure 5**).

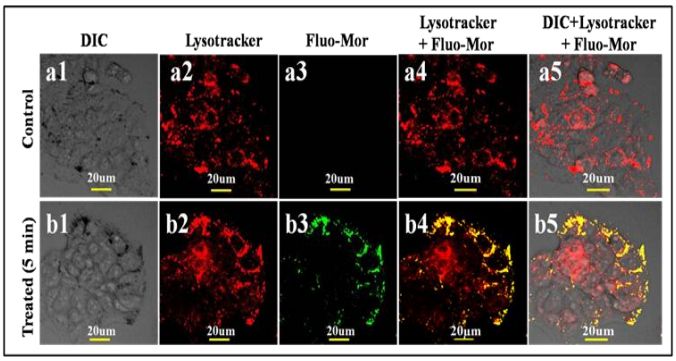

Figure 5 Lysosome localisation study using confocal microscopic images for human colon cancer HT-29 cell treated with and without Fluo-Mor NPs; shown are **(a)** untreated cells **(b)** cell treated with Fluo-Mor NPs; **(1)** bright-field images , fluorescence images **(2)** in the 590-nm (LysoTracker Red DND 99) and **(3)** 460-nm (Fluo-Mor NPs) emission channels, **(4)** overlays of the fluorescence images of lysotracker dye and Fluo-Mor NPs, **(5)** overlays of the bright-field images and the fluorescence images of lysotracker dye and Fluo-Mor NPs. Scale bar =20 µm

Photoinduced cytotoxicity of Fluo-Mor NPs by MTT assay

The cytotoxicity of the Fluo-Mor NPs was also tested in human colon cancer cell line HT-29 via 3-(4,5-dimethylthiazol-2-yl)-2,5-diphenyltetrazolium bromide assay (MTT assay).[29] The time-dependent study revealed that within 5 min of irradiation (≥365 nm) and subsequent incubation for 16 h, the cell viability decreased up to 30% (figure 6), in accordance with the result of the singlet oxygen generation study (figure 4). Further, a dose-dependent study revealed that at 75 µg/mL concentration, cell viability is maximum (~ 90 %) for the Fluo-Mor NPs, whereas it was only 37 % at a concentration of 300 µg/mL.

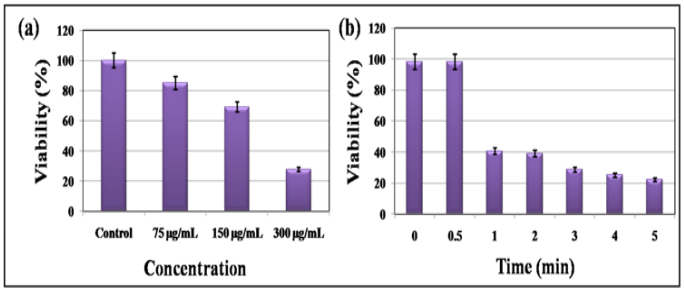

Figure 6 Comparative Cell viability study of Fluo-Mor NPs on Human Colon cancer HT-29 cells **(a)** dose-dependent and **(b)** time-dependent decrease of cell viability at a Fluo-Mor NPs concentration of 300 µg/mL under the irradiation of UV-vis light of ≥365 nm (fluence rate = 16 mW/cm^2). Values are presented as means ± standard deviations of three different observations.

Live/Dead assay for HT-29 colon cancer cell line by Fluo-Mor NPs

Further confirmation of cancer cell death was carried out by Live/Dead assay with Calcein AM and Ethidium homodimer-1. Calcein AM is a membrane permeable fluorogenic esterase substrate that is hydrolysed in live cells to yield cytoplasmic green fluorescence. Membrane-impermeable ethidium homodimer-1 labels nucleic acids of membrane-compromised dead cells with red fluorescence.[30] In **figure 7 (a2),** the untreated cells showed strong green fluorescence due to presence of cell permeable Calcein AM dye, however **figure 7 (a3)** showed absence of any significant staining by Ethidium homodimer-1, which indicated presence of live cells. After treating the HT-29 cells with Fluo-Mor NPs for 5 min using ≥ 365 nm wavelength, appearance of intense red fluorescence of Ethidium Homodimer-1 was observed (**figure 7 (b3)),** that implied loss of cancer cell membrane integrity or membrane rupture, characteristic behaviour of apoptotic cell death. Of note, the merged (yellow portions) portions indicated in **figure 7 (b4)** were suggestive of beginning of cell death process. Thus, from the live/dead assay, it could be inferred that the cell death process might be via apoptosis as reported in literature.[30]

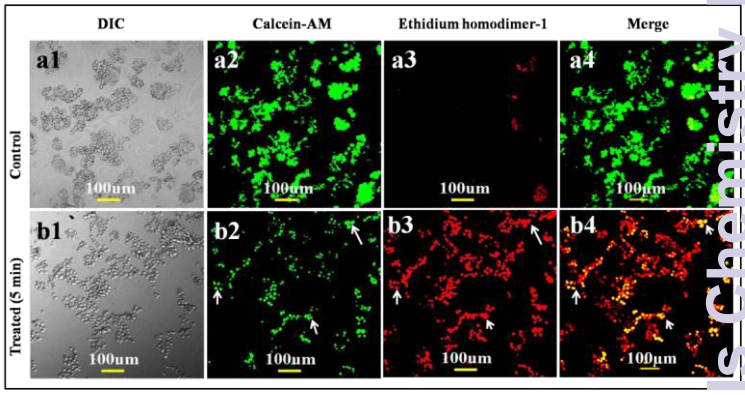

Figure 7 Live/Dead assay for HT-29 colon cancer cell line in presence of Fluo-Mor NPs; **(a)** before irradiation of light, **(b)** after 5 min of light irradiation; **(1)** bright-field images, **(2)** fluorescence image of Calcein AM at 520 nm, **(3)** fluorescence image of Ethidium Homodimer 1 at 617 nm and **(4)** overlays of the bright-field images and the fluorescence images. Scale bar =100 µm

DAPI staining for nuclear morphology observation

Nuclear morphology of cancer cell was studied by confocal imaging using nucleus-staining dye 4',6-diamidino-2-phenylindole (DAPI) (**supplementary fig. S7**).[31] Normal nuclei (smooth) and apoptotic nuclei (fragmented or condensed) were easily distinguished from this assay. **Supplementary fig. S7 (a2) and (b2)** showed the nuclear morphology upon drug treatment before and after photolysis. The nuclear morphology analysis by DAPI staining showed prominent nuclear fragmentation and condensation in colon cancer cells treated with Fluo-Mor NPs, indicating efficient cell destruction through apoptosis (**supplementary fig. S7 (b2)**). However,

cytotoxic effect of Fluo-Mor NPs upon light irradiation was evaluated in various ways but for further confirmation of apoptotic cell death additional studies would be required.

Intracellular singlet oxygen generation by Fluo-Mor NPs

Further, to qualitatively estimate the intracellular singlet oxygen generation by Fluo-Mor NPs, the colon cancer cell line was stained with dichloro-dihydro fluorescein diacetate (DCFH-DA).[32] DCFH-DA is a non-fluorescent molecule, whereas upon oxidation by reactive oxygen species (ROS) it is converted to dichloro fluorescein (DCF) which exhibits strong green fluorescence upon excitation at 488 nm. Hence, to explore the cell death pathway via PDT by Fluo-Mor NPs, the colon cancer cells were co-incubated with DCFH-DA and Fluo-Mor NPs (λ_{ex} = 365 nm, λ_{em} = 460 nm). Before irradiation, very less fluorescence was found for DCF (**figure 8 (c1)**), implying negligible singlet oxygen production. However, when the colon cancer cells were irradiated, generation of strong green fluorescence of DCF (λ_{ex} = 488 nm, λ_{em} = 530 nm) was observed (**figure 8 (c2-c3)**). Interestingly, the intracellular fluorescence intensity of DCF increased in presence of Fluo-Mor NPs upon irradiation of UV light (≥ 365 nm) in comparison to the control, which were measured and graphically represented with respect to irradiation time (**supplementary fig. S8**).

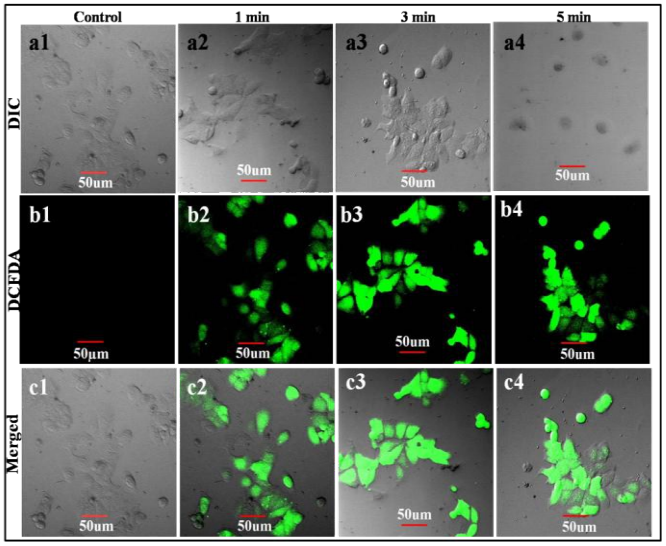

Figure 8 Intracellular generation of singlet oxygen by Fluo-Mor NPs using DCFH-DA assay. Shown are; **(a)** bright-field, **(b)** fluorescent and **(c)** merged images of bright-field and fluorescent images of **(1)** control cells with Fluo-Mor NPs in dark, **(2)** after 1 min, **(3)** 3 min and **(4)** 5 min of irradiation with light of ≥365 nm (16 mW cm^{-2})

Conclusion

In conclusion, we have developed a new organic NP for both diagnosis and treatment of cancer in a controlled and site-specific manner. Our newly designed Fluo-Mor NPs showed reversible fluorescence switch ON-OFF (ON= fluorescent; OFF= non-fluorescent) property which rendered real time monitoring of PDT activity. Moreover, as-synthesized NPs showed efficient PDT activity with a quantum yield of 0.65, controlled by both pH and light. Further, due to their small size (43 nm), the Fluo-Mor NPs were readily entered into cancer cells and showed selective singlet oxygen generation in the lysosomal cavity, indicated by DCFH-DA assay. MTT assay in human colon cancer cells revealed that the Fluo-Mor NPs were extremely efficient in cell destruction after 5 min of UV-vis irradiation. Our present strategy can be further extended towards the development of new organic NPs based on other renowned photosensitizers in near future.

Acknowledgements

Authors are thankful to DST-SERB for financial support and DST-FIST for 400 MHz NMR. Moumita Gangopadhyay is thankful to IIT KGP for the fellowship. We are thankful to Dr. Avijit Jana, School of Physical & Mathematical Sciences (SPMS) Nanyang Technological University for valuable suggestions.

Notes and references

1 J. L. Vivero-Escoto, D. DeCillis, L. Fritts and D. L. Vega, *Proc. SPIE,* 2014, **8931**, 89310Z-1.
2 J. Tian, L. Ding, H. J. Xu, Z.Shen, H. Ju, L. Jia, L. Bao and J. S. Yu, *J. Am. Chem. Soc.*, 2013, **135**, 18850.
3 S. Wang, R. Gao, F. Zhou and M. Selke, *J. Mater. Chem.,* 2004, **14**, 487.
4 A. Wiseman, Handbook of Enzyme Biotechnology, Horwood, Chichester, 1985.
5 W. Tang, H. Xu, R. Kopelman and M. A. Philbert, *Photochem. Photobiol.,* 2005, **81**, 242.
6 Y. N. Konan, J., Chevallier, R. Gurny and E. Alle´mann, *Photochem. Photobiol.,* 2003, **77**, 638.
7 G. Obaid, I. Chambrier, M. J. Cook and D. A. Russell, *Photochem. Photobiol. Sci.,* 2015, **14**, 737.
8 A. Khdair, D. Chen, Y. Patil, L. Ma, Q. P. Dou, M. P.V. Shekhar, J. Panyam, *J. Control. Release,* 2010, **141**, 137.
9 M. Wang, G. Abbineni, A. Clevenger, C. Mao and S. Xu, *Nanomed. Nanotech. Biol. Med.,* 2011, **7**, 710.
10 V. Milosavljevica, A. Moulicka, P. Kopela, V. Adama and R. Kizek, *Journal of Metallomics and Nanotechnologies,* 2014, **3**, 16.
11 N. Puvvada, D. Mandal, P. K. Panigrahi and A. Pathak, *Toxicol. Res.*, 2012, **1**, 196.
12 S. M. Lee, H. J. Kim, Y. J. Ha, Y. N. Park, S. K. Lee, Y. B. Park, and K. H. Yoo, *ACS Nano*, 2013, **7**, 50.
13 A. M. Nowicka, A. Kowalczyk, A. Jarzebinska, M. Donten, P. Krysinski and Z. Stojek, *Biomacromolecules*, 2013, 14, 828.
14 A. Valizadeh, H. Mikaeili, M. Samiei, S. M. Farkhani, N. Zarghami, M. kouhi, A. Akbarzadeh and S. Davaran, *Nanoscale Res. Lett.*, 2012, **7**, 480.
15 F. He, G. Yang, P. Yang, Y. Yu, R. Lv, C. Li, Y. Dai, S. Gai and J. Lin, *Adv. Funct. Mater.,* 2015, **25**, 3966.
16 D. Yang, G. Yang, S. Gai, F. He, G. An, Y. Dai, R. Lv and P. Yang, *Nanoscale*, 2015, **7**, 19568.
17 A. J. Gesquiere, T. Uwada, T. Asahi, H. Masuhara and P. F. Barbara, *Nano Lett.,* 2005, **5**, 1321.
18 M. M. K. Motlagh, R. Rahimi and M. J. Kachousangi, *Molecules*, 2010, **15**, 280.
19 A. Jana, K. S. P. Devi, T. K. Maiti and N. D. P. Singh, *J. Am. Chem. Soc.,* 2012, **134**, 7656.
20 H. Nakanishi and H. Katagi, *Supramol. Sci.*, 1998, **5**, 289.
21 L. Zhou, W. Wang, Y. Feng, S. Wei, J. Zhou, B. Yua, J. Shen, *Bioorg. Med. Chem. Lett.,* 2010, **20**, 6172.
22 M. Doshi, A. Copik and A. J. Gesquiere, *Photodiagnosis Photodyn. Ther.*, 2015, **12**, 476.

23 K. Baba, H. E. Pudavar, I. Roy, T. Y. Ohulchanskyy, Y. Chen, R. K. Pandey and P. N. Prasad, *Mol. Pharm.,* 2007, **4**, 289.
24 K. D. Belfield, C. C. Corredor, A. R. Morales, A. M. Dessources and F. E. Hernandez, *J. Fluoresc.,* 2006, **16**, 105.
25 C. L. Andrew, A. R. Klemm and J. B. Lloyd, *Biochim. Biophys. Acta,* 1997, **1330**, 71.
26 K. D. Belfield, K. J. Schafer, W. Mourad and B. A. Reinhardt, *J. Org. Chem.,* 2000, **65**, 4475.
27 Q. Zou, Y. Fang, Y. Zhao, H. Zhao, Y. Wang, Y. Gu and F. Wu, *J. Med. Chem.*, 2013, **56**, 5288.
28 A. Kamkaew and K. Burgess, *J. Med. Chem.* 2013, **56**, 7608.
29 S. Karthik, N. Puvvada, B. N. Prashanth Kumar, S. Rajput, A. Pathak, M. Mandal and N. D. Pradeep Singh, *ACS Appl. Mater. Interfaces* 2013, **5**, 5232.
30 N. P. Matylevitch, S. T. Schuschereba, J. R. Mata, G. R. Gilligan, D. F. Lawlor, C. W. Goodwin, P. D. Bowman, *Am. J. Pathol.,* 1998, **153**, 567.
31 M. J. Marín, F. Galindo, P. Thomas, T. Wileman and D. A. Russell, *Anal. Bioanal. Chem.,* 2013, **405**, 6197.
32 S. R. Tsai, R. Yin, Y. Y. Huang, B. C. Sheu, S. C. Lee, M. R. Hamblin, *Photodiagnosis Photodyn. Ther.* 2015, **12**, 123.
33 Y. Hu, T. Litwin, A. R. Nagaraja, B. Kwong, J. Katz, N. Watson and D. J. Irvine, *Nano Lett.*, 2007, **7**, 3056.
34 T. C. Prathna, N. Chandrasekaran and A. Mukherjee, *Colloids and Surfaces A: Physicochem. Eng. Aspects*, 2011, **390**, 216.
35 C. S. Lee, W. Park, Y. U. Jo and K. Na, *Chem. Commun.,* 2014, **50**, 4354.
36 P. Xu, E. A. Van Kirk, Y. Zhan, W. J. Murdoch, M. Radosz, Y. Shen, *Angew. Chem. Int. Ed.,* 2007, **46**, 4999.
37 Z. Zhou, Y. Shen, J. Tang, E. Jin, X. Ma, Q. Sun, B. Zhang, E. A. Van Kirk and W. J. Murdoch, *J. Mater. Chem.,* 2011, **21**, 19114.
38 J. Z. Du, T. M. Sun, W. J. Song, J. Wu and J. Wang, *Angew. Chem. Int. Ed.*, 2010, **49**, 3621.
39 N. Ghinea and N. Simionescu, *J. Cell Biol.*, 1985, **100**, 606.
40 H. Fu, *Dyes and Pigments*, 2015, **115**, 211.
41 Z. Chen, J. Liang, X. Han, J. Yin, G. A. Yu, S. H. Liu. Dyes *and Pigments,* 2015, **112**, 59.
42 S. J. Ananthakrishnan, E. Varathan, E. Ravindran, N. Somanathan, V. Subramanian, A. B. Mandal, J. D. Sudhacd and R. Ramakrishnan, *Chem. Commun.*, 2013, **49**, 10742.
43 X. J. Jiang, P. C. Lo, S. L. Yeung, W. P. Fong and D. K. P. Ng, *Chem. Commun.*, 2010, **46**, 3188.
44 X. Zhu, W. Lu, Y. Zhang, A. Reed, B. Newton, Z. Fan, H. Yu, P. C. Ray and R. Gao, *Chem. Commun.*, 2011, **47**, 10311.
45 A. Ogunsipe, D. Maree and T. Nyokong, *J. Mol. Struct.*, 2003, **650**, 131.

Fluorene-Morpholine based Organic Nanoparticles : Lysosome-targeted pH-triggered Two-photon Photodynamic Therapy with Fluorescence Switch On-Off

Moumita Gangopadhyay,[a] Sourav K. Mukhopadhyay,[b] Sree Gayathri,[a] Sandipan Biswas,[a] Shrabani Barman,[a] Satyahari Dey,*[b] N D Pradeep Singh*[a]

.

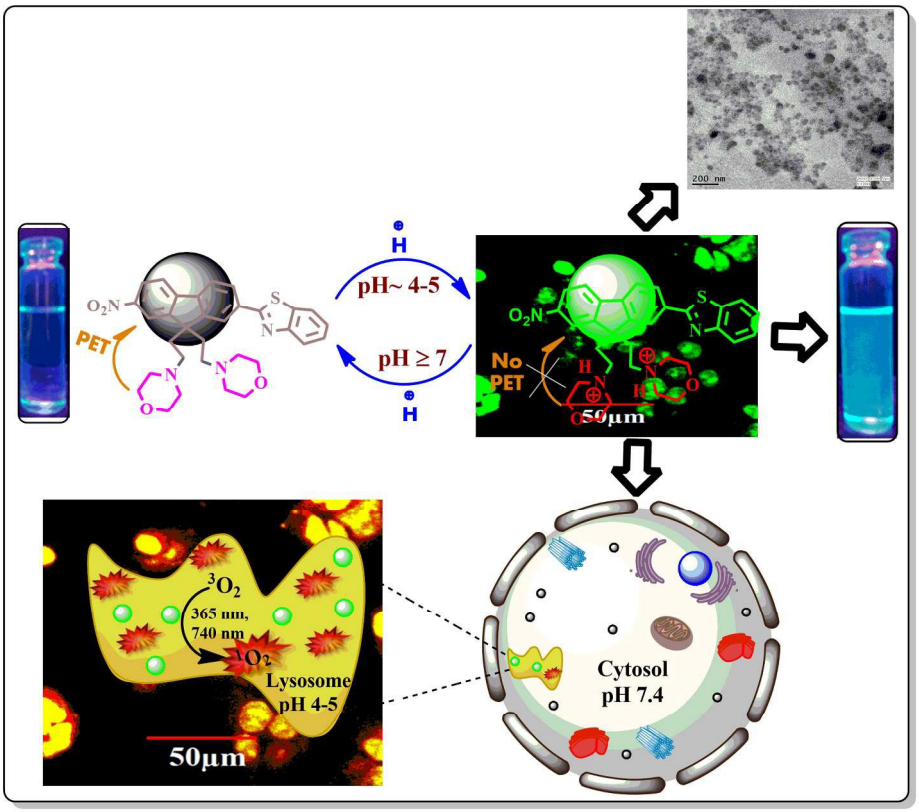

We synthesized Fluorene-Morpholine NPs that showed reversible fluorescence switch ON-OFF property which rendered real time monitoring of PDT activity.